

Supporting Information

A Soft On/Off Switch Based on the Electrochemically Reversible H-J Interconversion of a Floating Porphyrin Membrane

Andrés F. Molina-Osorio,^a Sho Yamamoto,^b Alonso Gamero-Quijano,^a Iván Robayo-Molina,^a Hirohisa Nagatani^{b,c} and Micheál D. Scanlon.^{*,a,d}

^a The Bernal Institute and Department of Chemical Sciences, School of Natural Sciences, University of Limerick (UL), Limerick V94 T9PX, Ireland

^b Division of Material Chemistry, Graduate School of Natural Science and Technology, Kanazawa University, Kakuma, Kanazawa 920-1192, Japan

^c Faculty of Chemistry, Institute of Science and Engineering, Kanazawa University, Kakuma, Kanazawa 920-1192, Japan

^d The Advanced Materials and Bioengineering Research (AMBER) centre, Dublin, Ireland

E-mail: * micheal.scanlon@ul.ie (M.D. Scanlon)

Table of Contents

| | | |
|-------------|--|------------|
| S1 | Experimental methods | S2 |
| S1.1 | Chemicals | S2 |
| S1.2 | Self-assembly of the zinc porphyrin membrane (ZnPor membrane) | S2 |
| S1.3 | Electrochemical measurements | S3 |
| S1.4 | <i>In situ</i> UV/vis spectroscopy in total internal reflection (TIR-UV/vis) at the bare ITIES and the membrane organic electrolyte interface. | S4 |
| S1.5 | Minimising baseline drift and artifacts for TIR-UV/vis absorbance measurements. | S5 |
| S1.6 | Polarisation-modulation total internal reflection fluorescence (PM-TIRF) measurements at the ITIES. | S8 |
| S2 | Supporting Figures | S9 |
| S3 | Supporting References | S14 |

S1. Experimental methods

S1.1 Chemicals. All reagents were used as received without further purification. Zinc *meso*-tetrakis(4-carboxyphenyl)porphyrin (ZnPor, $\geq 98\%$) was obtained from Porphychem. Lithium hydroxide (LiOH, $\geq 98\%$), citric acid (H_3Cit , $\geq 99.5\%$), bis(triphenylphosphoranylidene) ammonium chloride (R_2NCl , 97%), tetrabutylammonium chloride (TBACl, $\geq 97\%$), tetraocylammonium chloride (TOACl, $\geq 98\%$) and cetyltrimethylammonium chloride (CTACl, $\geq 98\%$) were purchased from Sigma-Aldrich. Lithium tetrakis(pentafluorophenyl)borate diethyletherate (LiTB) was purchased from Boulder scientific, and α,α,α -trifluorotoluene (TFT, $\geq 99\%$) from Acros Organics. All aqueous solutions were prepared using Milli-Q® deionized water (18.2 M Ω). Aqueous solutions of ZnPor were prepared by directly dissolving the solid in the lithium citrate buffer pre-adjusted to the desired pH, followed by sonication of the solution for three minutes.

The organic electrolyte was obtained by a metathesis reaction between R_2NCl and LiTB. In a typical procedure, equimolar quantities of LiTB and R_2NCl were dissolved separately in a mixture of $\text{CH}_3\text{OH}:\text{H}_2\text{O}$ 2:1 (v/v). The solutions obtained were mixed together and stirred for 30 minutes at room temperature. After this time, a white powder in suspension was obtained. This suspension was then filtered and the solid obtained collected in a beaker. Acetone was added drop-wise to this solid until most of it was dissolved. The solution obtained was filtered again and water was added drop-wise to precipitate the solid. The acetone in the mixture was then evaporated by gently heating (50°C) and stirring. The solid obtained was pure R_2NTB , and vacuum dried for two hours to obtain a fine white powder. The organic salts TBATB, CTATB and TOATB were prepared using the same procedure.

S1.2 Self-assembly of the zinc porphyrin membrane (ZnPor membrane). The porphyrin membrane self-assembled from aqueous solutions of 10 μM of ZnPor. The self-assembly was carried out at the water|TFT interface for 30 minutes. Critically, the pH of the aqueous solution was adjusted using a 10 mM Li_2HCit (lithium citrate buffer) to match the pK_a of the 4-carboxyphenyl substituents ($\text{pK}_a^{\text{COOH}} = 5.8$).¹ Subsequently, this solution was contacted with TFT (an organic solvent that is immiscible with water) for 30 minutes, leading to the formation of a well-defined aqueous|organic interface. Upon contact, the clear formation of interfacial nanostructures was immediately seen visually. The water|TFT interface took on a yellow/green

complexion, easily distinguishable from the purple colour of bulk ZnPor aqueous solution. The intensity of the interfacial colouration increased with time, ultimately leading to the formation of a ZnPor membrane. For cyclic voltammetry and *in situ* TIR-UV/vis absorbance experiments, porphyrin not adsorbed at the interface was carefully removed and replaced with Li₂HCit buffer. This procedure was repeated until no porphyrin was detectable by UV/vis spectroscopy in the aqueous phase.

S1.3 Electrochemical measurements. Electrochemical measurements at the interface between two immiscible electrolyte solutions (ITIES) were carried out with a PGSTAT204 Autolab Metrohm potentiostat using a four-electrode electrochemical cell (see **Fig. S1**). The reference electrodes used were Ag/AgCl for the organic side and Ag/AgCitrate(Ag₃Cit) for the aqueous side. The counter electrodes were Pt. The electrolyte in the aqueous phase was a 10 mM buffer of Li₂HCit at different pH values. In the organic phase, the solvent used was TFT, and the organic electrolyte was 5 mM R₂NTB. The electrochemical cell configuration investigated in this communication is presented in **Fig. S1a**, where each vertical line represents a phase boundary and the double vertical line represents the polarisable interface between the membrane and the aqueous and organic electrolyte solutions.

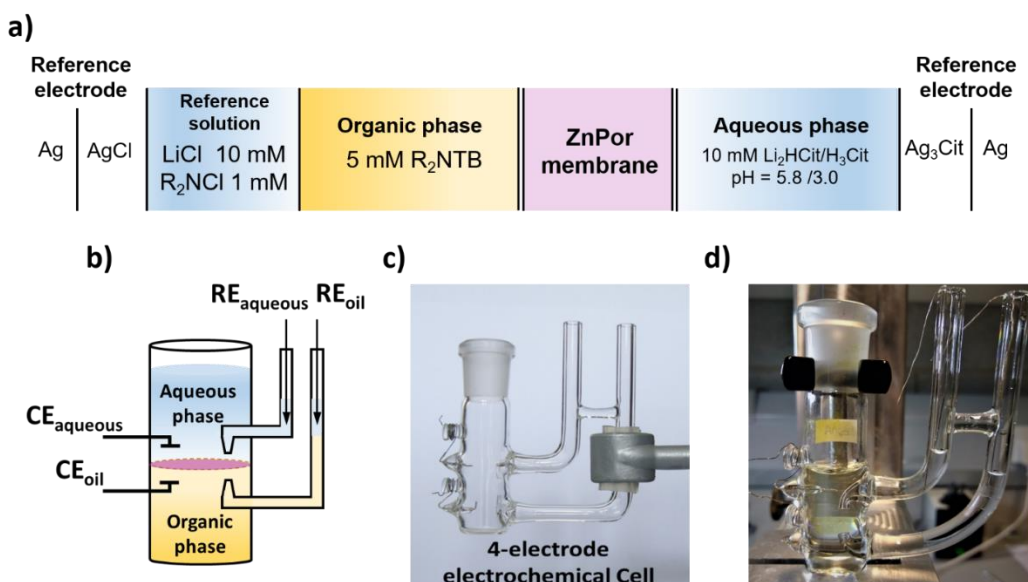


Fig. S1. (a) Four-electrode electrochemical cell configuration used for electrochemical measurements. (b) Schematic, (c) and (d) pictures of the cell. CE = counter electrode, RE = reference electrode. R₂N = bis(triphenylphosphoranylidene)ammonium cation. TB = tetrakis(pentafluorophenyl)borate anion. Organic solvent = α,α,α -trifluorotoluene.

S1.4 *In situ* UV/vis spectroscopy in total internal reflection (TIR-UV/vis) at the bare ITIES and the membrane|organic electrolyte interface. In order to analyse the effect of the applied interfacial Galvani potential difference ($\Delta\phi^w$) on the structure of the ZnPor membrane, *in situ* TIR-UV/Vis absorbance at the polarised water|TFT and membrane|TFT interfaces was used. In this configuration, the light source was directed towards the interface with the aid of focusing lenses, diaphragm and mirrors (see **Fig. S2**) at an angle of incidence (AOI) calculated using Snell's law and the refractive indexes of water ($\eta_{\text{H}_2\text{O}}$) and TFT (η_{TFT}) as follows:

$$\eta_{\text{TFT}} \sin\theta_1 = \eta_{\text{H}_2\text{O}} \sin\theta_2$$

If θ_2 is assumed to be 90°

$$\theta_2 = 90^\circ$$

$$\sin \theta_2 = 1$$

Applying Snell's law, with $\eta_{\text{H}_2\text{O}}$ and η_{TFT} equal to 1.330 and 1.414, respectively, the critical angle was determined as follows:

$$\sin \theta_1 = \frac{\eta_{\text{H}_2\text{O}}}{\eta_{\text{TFT}}} = \frac{1.330}{1.414} = 0.940$$

$$\theta_1 = \sin^{-1}(0.940) = 70.05^\circ$$

The light source (Xe lamp HPX-2000, Ocean Optics) was guided by an optical fiber with a 200 μm core (Newport) and focused on the water|TFT and membrane|TFT interfaces through plano-convex (Thorlabs) and achromatic lenses (Newport), see **Fig. S2**. All lenses were placed at their confocal lengths. The longer wavelengths ($\lambda > 700 \text{ nm}$) were cut by a Hot Mirror (Thorlabs) to avoid heating of the interfacial region. The reflected light was focused onto an optical fiber with a 1500 μm core (Thorlabs). The AOI to the interface was set as 75° . A neutral density (ND) filter (Thorlabs) was used to reduce the intensity of the light beam; the ND filter was placed directly after the source to avoid photobleaching of the porphyrin. The absorption spectra were recorded by a Maya 2000Pro (Ocean Optics).

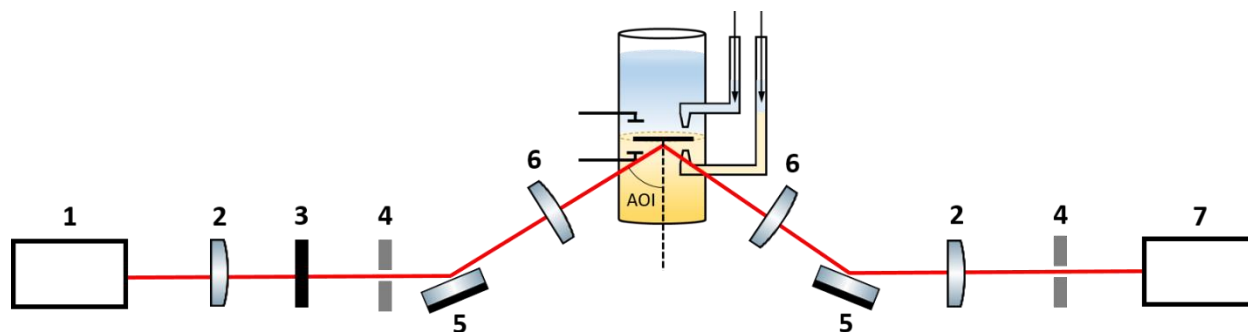


Fig. S2. Optical setup for *in situ* UV/vis absorbance measurements in total internal reflection (TIR-UV/vis absorbance). (1) Xe light source (Ocean optics HPX-2000), (2) UVFS coated plano convex lenses, (3) neutral density (ND) filter, (4) iris diaphragm, (5) “Hot” mirror (cut-off wavelength 800 nm), (6) Achromatic doublets, and (7) Ocean Optics Maya2000 Pro spectrometer. The angle of incidence (AOI) was set to 75° .

S1.5 Minimising baseline drift and artifacts for TIR-UV/vis absorbance measurements. The baseline for the TIR-UV/vis absorbance measurements was affected by heating of the interface with infrared radiation and changes in the surface tension at different $\Delta\phi_w$.² To minimise the former, a hot mirror was placed between the light source and the interface. As presented in **Fig. S3a**, the hot mirror effectively cut off wavelengths in the infrared region above 700 nm. Using this configuration, the drifting of the spectral baseline was significantly reduced over time and no artifact was observed in the region of interest (see **Fig. S3b**).

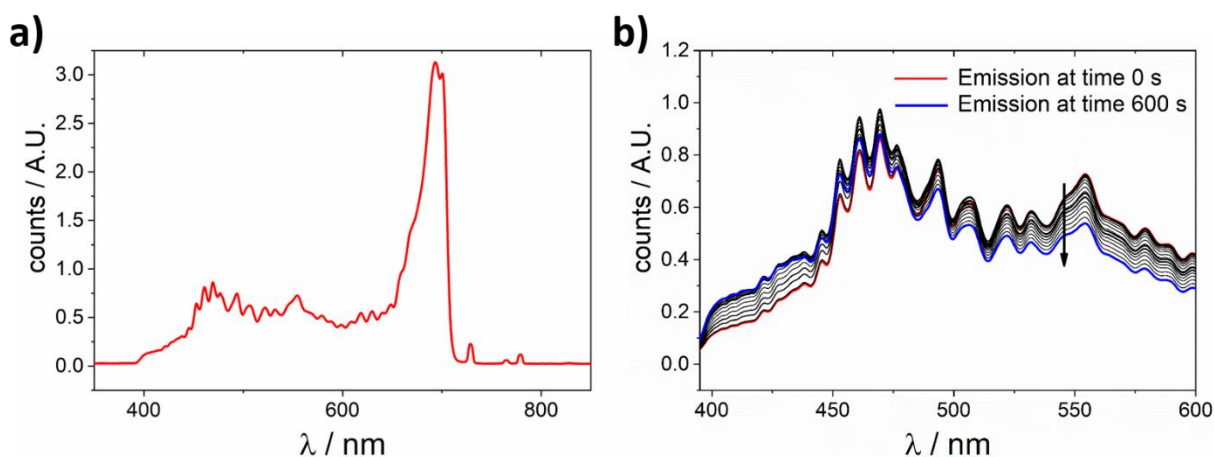


Fig. S3. Xe lamp emission after being reflected at the water|TFT interface. (a) Emission using a “hot” mirror that cuts off wavelengths above 700 nm. (b) Variation of the emission spectra over a 10 minutes period. Spectra were taken every 60 seconds.

The effect of the polarisation potential on the baseline drift and possible spectral artifacts was analysed at the ITIES in the absence of the ZnPor membrane at the interface. The CV recorded under these conditions shows no electrochemical signals in a potential range between -0.2 and 0.6 V (see **Fig. S4a**). Additionally, taking as a reference the spectrum at $+0.40$ V, *in situ* TIR-UV/vis spectra at different potentials presented in **Fig. S4b** show only small variations in the spectral baseline at $+0.4$ and $+0.2$ V. At -0.25 and -0.30 V, some baseline drift at the bare liquid|liquid interface was observed. However, as conclusively shown *vide infra* in **Fig. S12**, the presence of the ZnPor membrane stabilises the interface with no baseline shift observed in the presence of the latter at negative applied potentials. Furthermore, no significant variations over time were observed for the spectral baseline at each of the potentials used in the analysis as presented in **Figs. S4c** and **S5**. Any variations are in the order of 0.005 A.U. and represent only 5 to 10% of the spectral shifts observed in the presence of the ZnPor membrane.

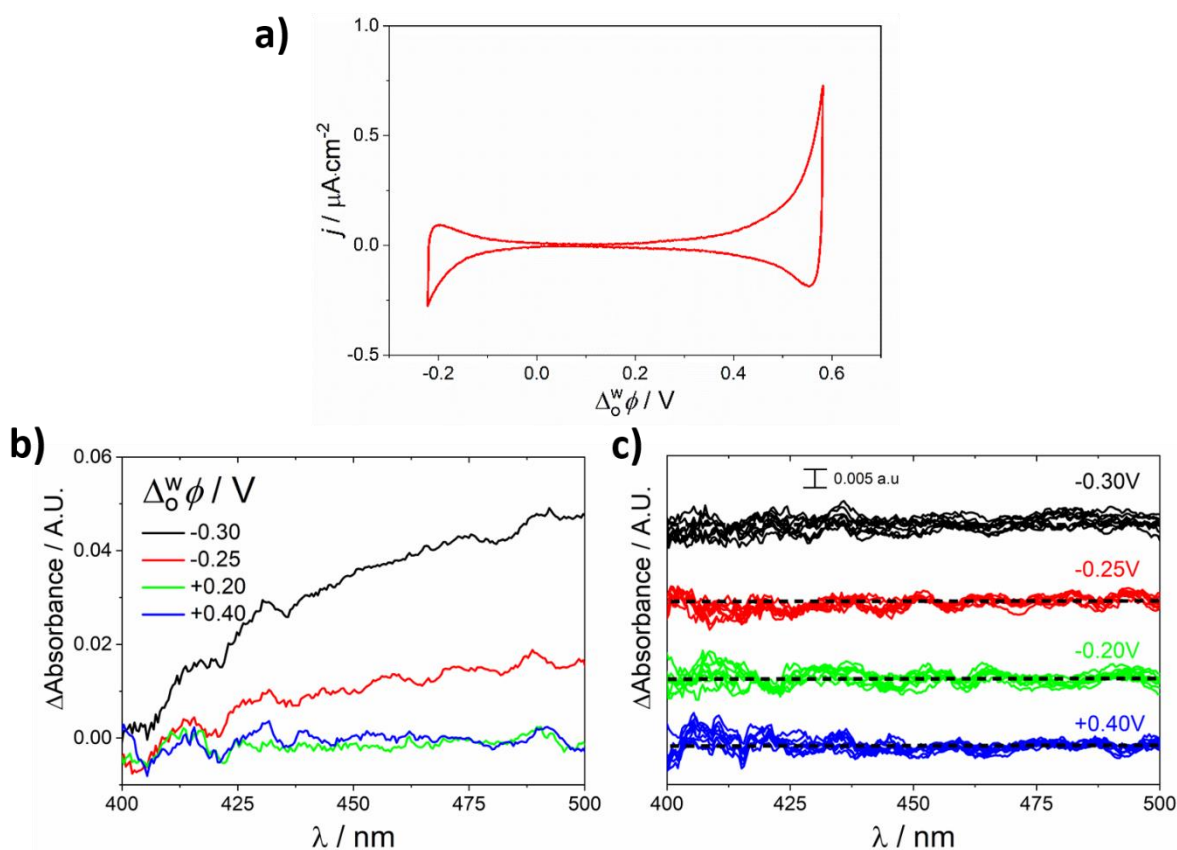


Fig. S4. Stability of the spectral baseline for *in situ* TIR-UV/vis experiments at different $\Delta_0^w \phi$ in the absence of the ZnPor membrane. (a) CV obtained in the absence of the ZnPor membrane using the configuration of the 4-electrode electrochemical cell employed outlined in **Fig. S1a**. The scan rate used was $20 \text{ mV} \cdot \text{s}^{-1}$ and the pH of the aqueous phase was 5.8. (b) Raw baseline obtained during *in situ* TIR-UV/vis absorbance experiments at different $\Delta_0^w \phi$, taking as a reference the spectrum obtained at $+0.40$ V. (c) Influence of time on the spectral baseline drift during *in situ* TIR-UV/vis experiments at different $\Delta_0^w \phi$. Spectra were taken at 6 second intervals for one minute and the first spectra (at $t = 0$) was used as the reference.

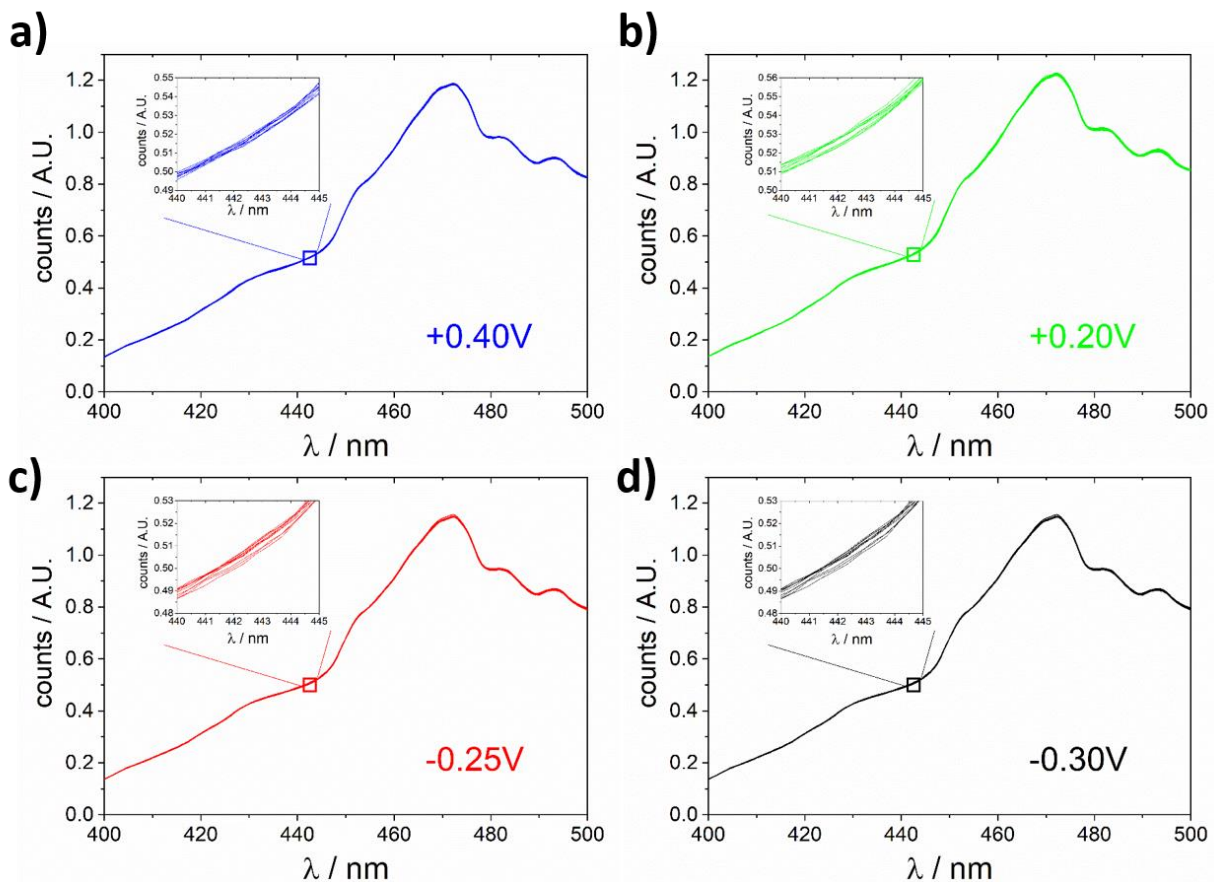


Fig. S5. The variation of Xe light source emission spectra after being reflected at the water|TFT interface polarized at different $\Delta_0^w \phi$. For each potential, the spectra were taken at 6 second intervals for one minute. Insets show a magnification region demonstrating the minimal variation of the spectra over time.

S1.6 Polarisation-modulation total internal reflection fluorescence (PM-TIRF) measurements at the ITIES. Periodic modulation between the p- and s-polarised incident beams was performed by a liquid crystal retarder (LCR) (Thorlabs, LCC1111T-A, LCC25/TC200) at 13 Hz. The excitation light source was a cw laser diode at 404 nm (Coherent, CUBE 405-50C). The output power was attenuated to < 25 mW to avoid photobleaching of ZnPor. The AOI was approximately 75° . The fluorescence signal from the interfacial region was measured perpendicularly to the interface by an optical fiber and a monochromator equipped with a photomultiplier tube (Shimadzu, SPG-120S), see **Fig. S6**. The polarisation-modulated fluorescence signal from the interfacial region was analysed by a digital lock-in amplifier (NF, LI5640) as a function of modulation frequency of the incident beam. The polarization-modulation efficiency (P_m) of LCR was obtained as 0.95 at 404 nm, indicating that 5 % of the s-polarized component remain in the p-polarized mode of LCR or *vice versa*.³

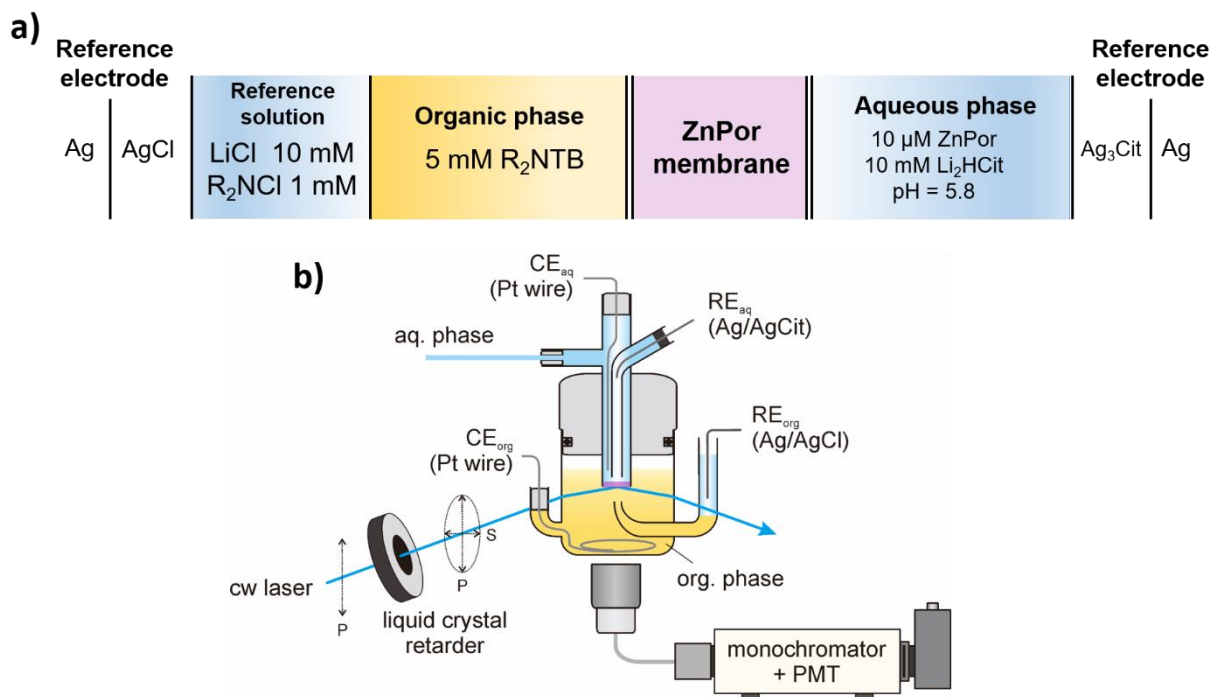


Fig. S6. (a) Schematic representation and (b) experimental setup of the spectroelectrochemical cell for PM-TIRF experiments.

S2. Supporting Figures

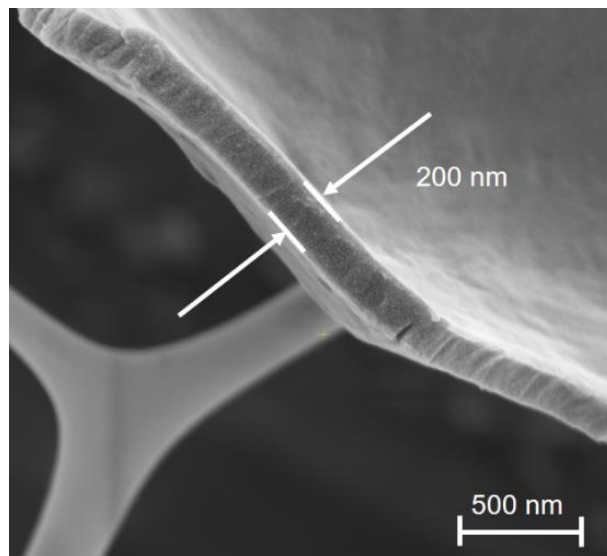


Fig. S7. Scanning electron microscopy (SEM) image of a ZnPor membrane transferred from the water|TFT interface to a copper grid with a holey carbon substrate. Images were obtained on a FEI Quanta 650 FEG high resolution SEM.

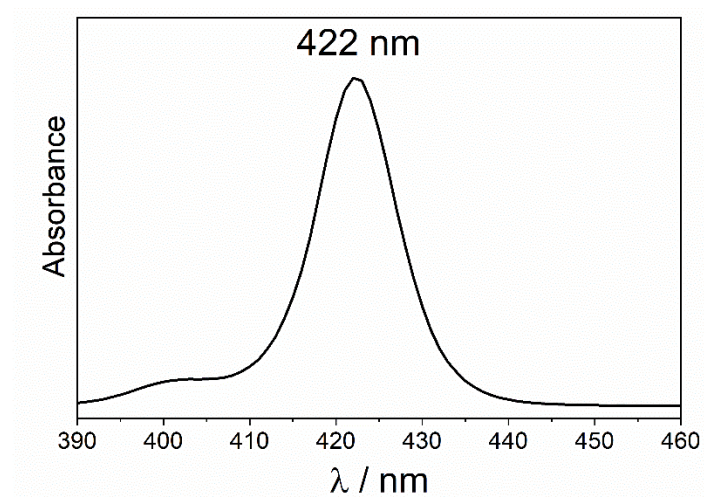


Fig. S8. UV/vis absorption spectrum of 10 μM ZnPor in an aqueous solution at pH 5.8.

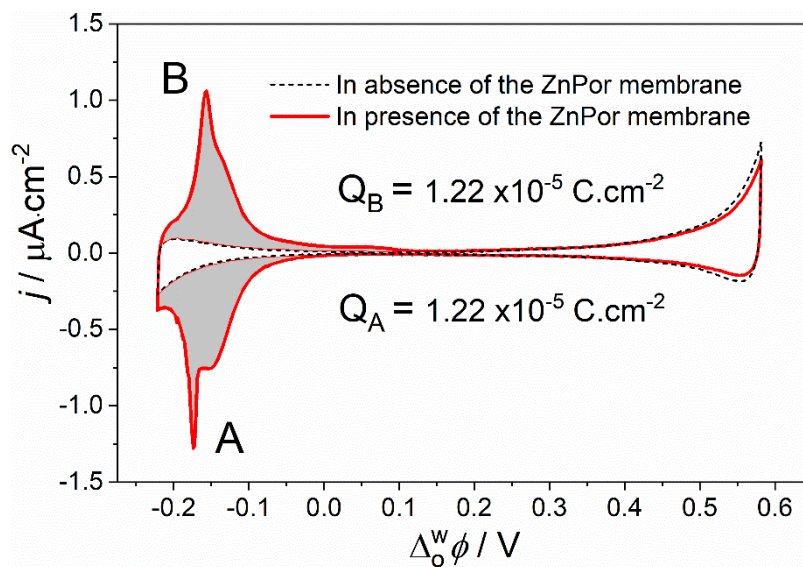


Fig. S9. Charge measured for each of the peaks observed in the presence of the ZnPor membrane. The configuration of the 4-electrode electrochemical cell employed is outlined in Fig. S1a. The scan rate used was $5 \text{ mV} \cdot \text{s}^{-1}$ and the start potential was $+0.30 \text{ V}$.

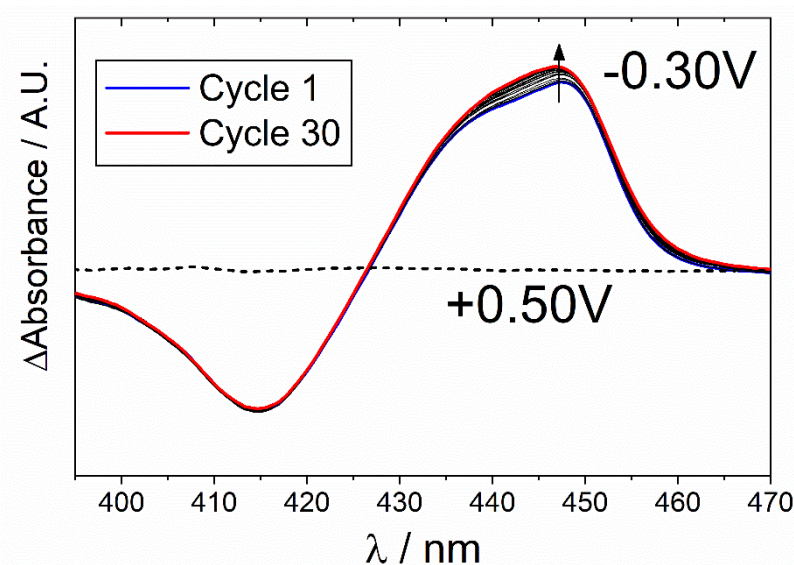


Fig. S10. Differential *in situ* TIR-UV/vis absorbance spectra of the ZnPor membrane as a function of the potential cycle number. The potential difference between the two electrolyte solutions was stepped between $+0.50$ and -0.30 V and back to $+0.50 \text{ V}$ during a single cycle. An animation of the change in the differential *in situ* TIR-UV/vis absorbance spectra with potential cycling is provided as an additional supporting information movie file.

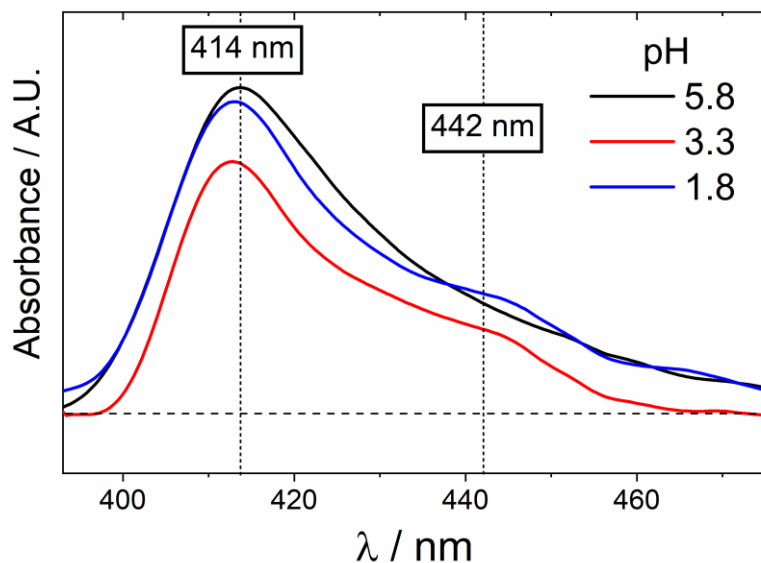


Fig. S11. *In situ* TIR-UV/vis absorbance spectra of a ZnPor membrane self-assembled from 50 μM ZnPor in solution at pH 5.8 for 30 minutes at open circuit potential (OCP). After self-assembly, the pH of the aqueous phase was adjusted to progressively more acidic pH values.

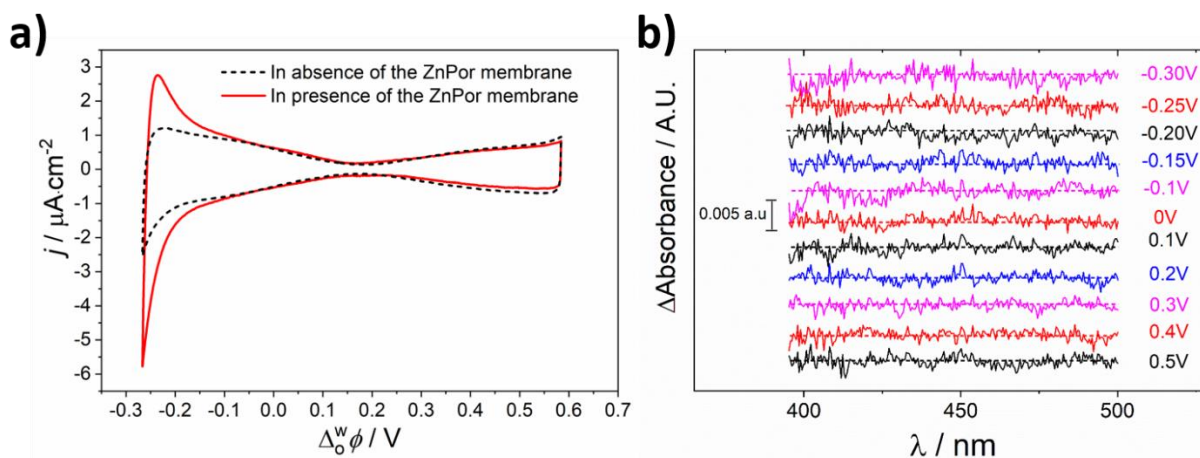


Fig. S12. pH suppression of the ion intercalation/exchange. (a) CV at $25 \text{ mV} \cdot \text{s}^{-1}$ obtained in the presence and absence of the ZnPor membrane at pH 3.0 using the configuration of the 4-electrode electrochemical cell employed outlined in Fig. S1. (b) Differential *in situ* TIR-UV/vis absorbance spectra of the ZnPor membrane at pH 3.0 and at different applied $\Delta_0^w \phi$. The spectrum of the ZnPor membrane at +0.50 V was taken as the baseline.

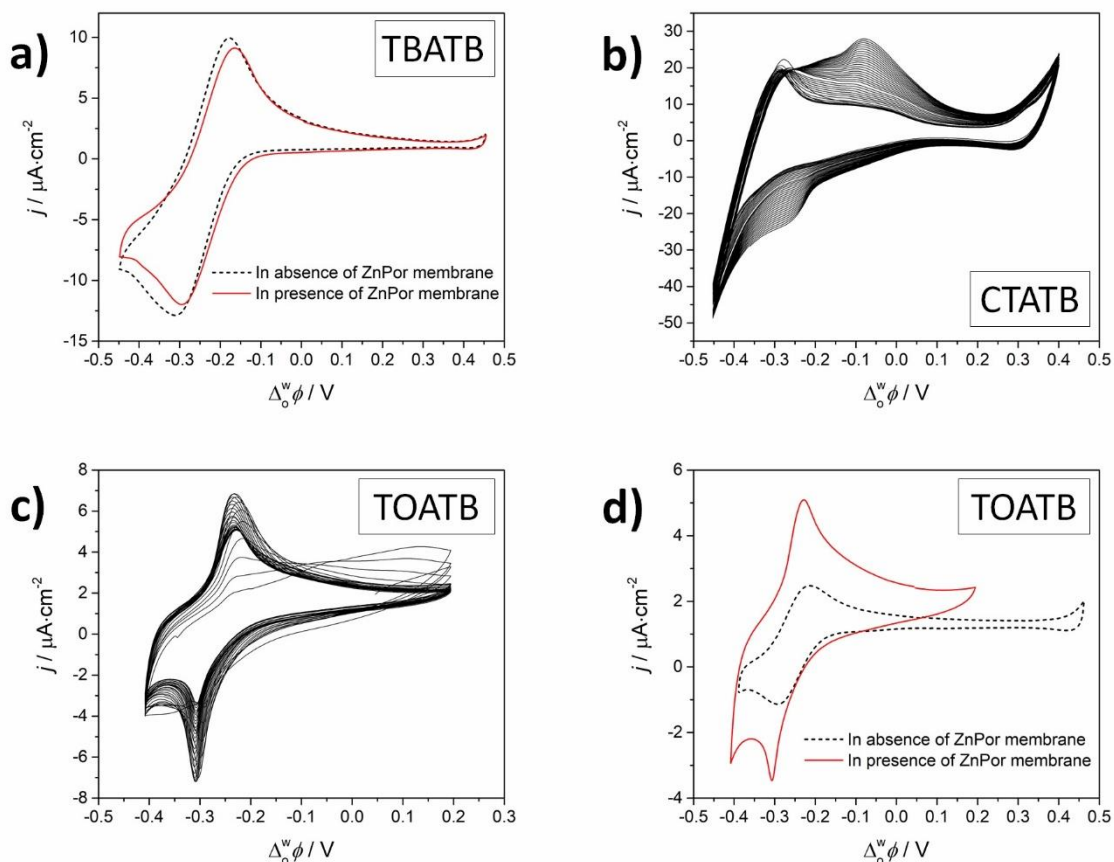


Fig. S13. CVs in the presence of alternative organic cations. (a) The configuration of the 4-electrode electrochemical cells employed were as described in Fig. S1a. with (a) 5 mM R_2NTB and 0.1 mM TEATB in the organic phase (scan rate used was $10 \text{ mV}\cdot\text{s}^{-1}$), (b) 5 mM CTATB in the organic (scan rate used was $50 \text{ mV}\cdot\text{s}^{-1}$), and (c) and (d) 5 mM TOATB in the organic phase (scan rate used was $10 \text{ mV}\cdot\text{s}^{-1}$).

R_2N^+ cations possess a number of features that facilitate their intercalation, leading to the ZnPor membrane interconverting from an H- to a J-type molecular configuration. R_2N^+ is a hydrophobic organic cation, and thus soluble in the organic solvent. Critically, R_2N^+ is sufficiently bulky to disrupt the structure of the ZnPor membrane such that changes in the TIR-UV/vis spectra are observed. Experiments with much less bulky TBA^+ cations in Fig. S13a did not demonstrate any evidence of intercalation. Instead, CVs in the presence (dashed black line, Fig. S13a) and absence (solid red line, Fig. S13a) of the ZnPor membrane were near identical as these relatively small cations permeate through the ZnPor membrane unimpeded and undergo reversible ion transfer to the aqueous phase. Indeed, only 0.1 mM TBA^+ was present in the organic phase in Fig.

S13a, as using 5 mM TBA⁺ would reduce the size of the potential window dramatically due to the massive current associated with TBA⁺ ion transfer.

Switching to the bulkier CTA⁺ (Fig. S13b) and TOA⁺ (Fig. S13c and d) organic cations was more successful, both producing CVs with peaks that increased in magnitude with successive CV scans and were reminiscent of those seen with R₂N⁺. In particular, the sharp peaks associated with the intercalation process were clearly seen with TOA⁺, highlighting the need for bulky cations to enable intercalation. In contrast to R₂N⁺, which does not transfer within the potential window at the ITIES, the applied $\Delta_0^w\phi$ for the intercalation peak of TOA⁺ (solid red line, Fig. S13d) matched its ion transfer potential (dashed black line, Fig. S13d). We speculate that the intercalation of R₂N⁺ may be facilitated by the ZnPor membrane. In other words, the intercalation process takes place at an applied $\Delta_0^w\phi$ more positive than R₂N⁺'s standard ion transfer potential. We attribute this to R₂N⁺'s aromatic nature and associated enhanced ability to disrupt π - π interactions in the ZnPor membrane. The TOA⁺ cations cannot interact with the ZnPor membrane by π - π interactions and undergo intercalation “directly” at an applied $\Delta_0^w\phi$ matching TOA⁺'s standard ion transfer potential.

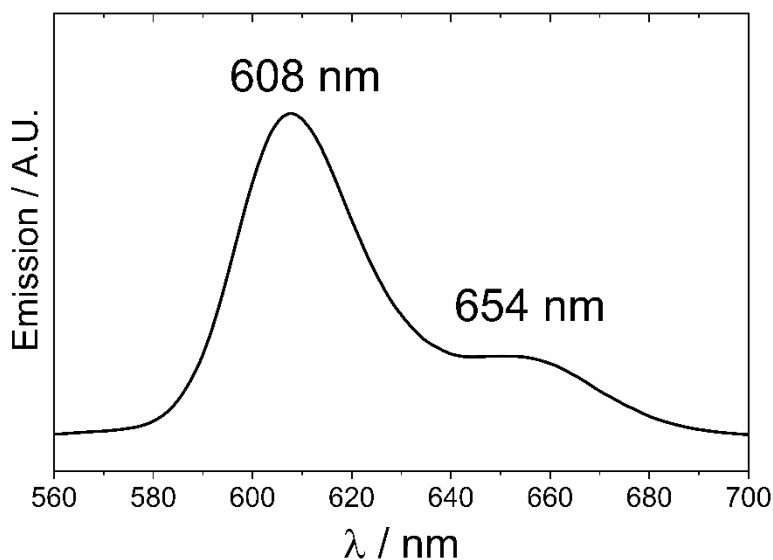


Fig. S14. Fluorescence emission spectrum of ZnPor in an aqueous solution, with [ZnPor] = 50 μ M and a pH of the aqueous phase of 5.8. The excitation wavelength was 418 nm.

S3. Supporting References

- 1 N. C. Maiti, S. Mazumdar and N. Periasamy, *J. Phys. Chem. B*, 1998, **102**, 1528–1538.
- 2 M. F. Suárez-Herrera and M. D. Scanlon, *Electrochim. Acta*, 2019, **328**, 135110.
- 3 S. Yamamoto, H. Nagatani, K. Morita and H. Imura, *J. Phys. Chem. C*, 2016, **120**, 7248–7255.